ARTICLE

Nano-porous Composites Based on Heteropolyacid Functionalized Ionic Liquid: Synthesis, Characterization, and Catalytic Performance in Esterification

Fu-dong Zhou[a], Wei Chu[a,b]*, Xiao-yan Dai[a], Shi-zhong Luo[a]

a. Department of Chemical Engineering, Sichuan University, Chengdu 610065, China
b. Key Lab of Green Chemistry and Technology of Ministry of Education, Sichuan University, Chengdu 610064, China

(Dated: Received on March 16, 2010; Accepted on April 26, 2010)

Functionalized ionic liquid samples (bmim-PW_{12}) were synthesized by 1-butyl-3-methyl-imidazolium bromide (bmimBr) and 12-phosphotungstic heteropolyacid (PW_{12}). The samples were annealed at 100−450 °C and were characterized by Fourier transform infrared spectroscopy, X-ray diffraction, scanning electron microscope, thermal gravity-DTG, brunauer emmett teller, and NH_3-temperature programmed desorption. The results showed that the bmim-PW_{12} samples were crystal and maintained intact Keggin structure. The organic parts of those samples were partly decomposed at a temperature more than 350 °C. The sample annealed at 400 °C exhibited nano-porous structure, strong acidity, and excellent catalytic activity on the esterification of *n*-butanol with acetic acid. The higher ester yield was obtained when the mass ratio of catalyst over the reactants amount was 5% for bmim-PW_{12} catalyst annealed at 400 °C.

Key words: Ionic liquid, 1-Butyl-3-methyl-imidazolium bromide, Phosphotungstic heteropolyacid, Annealing treatment, Esterification

I. INTRODUCTION

The room temperature ionic liquids (RTILs) are referred as "designer green solvents and catalysts". They exhibit fascinating properties *i.e.* good chemical and thermal stability, non-volatility, excellent electrochemical performances, and nonflammability *etc.* [1−3]. RTILs have attracted intensive interests in fundamental researches and applications, including potential templates for the synthesis of novel materials, solvents in chemical reactions and so on [1, 3−9]. Heteropolyacids are important acids with strong Brønsted acidity and their special Keggin anions are in the structure of $XM_{12}O_{40}{}^{n-}$ (M=W, Mo; X=P, Si). The combination of organic cation of common ionic liquid with heteropolyanion could synthesize a novel kind of ionic liquid. In fact, only a few new ionic liquids (*e.g.*, $[C_n\text{mim}]_3PW_{12}O_{40}$, $[(n\text{-}C_4H_9)_4N]_4S_2M_{18}O_{62}$ (M=Mo, W; n=2, 5; mim=methylimidazolium)) were reported in previous references [10−13], and they were used as electrochemicals rather than catalysts.

Acid-catalyzed esterification reactions have been widely used to get arylic, aliphatic and heterocyclic esters, which are significant intermediates in chemical and pharmaceutical industries [14]. In the beginning period, esterification reactions were usually catalyzed by some mineral acids, such as sulphuric acid, hydrogen chloride as well as orthophosphoric acid. However, there were environmental pollutions for these traditional catalysts. Therefore, heterogeneous catalysts, such as supported mineral acids [15], metal salts [16] as well as zeolites [17], were used in esterifications. Unfortunately, these catalysts have the disadvantages of deactivation and loss during the esterification reaction. Considering economic and environmental reasons, chemists should produce the desired product in a high yield and a good reusability through a safe and green process [18]. Hence, we designed novel heteropolyanion-functional ionic liquids as catalysts for acid-catalyzed esterification reactions.

In this work, novel heteropolyanion-functionalized ionic liquids (bmim-PW_{12}) were synthesized by using 12-phosphotungstic acid ($H_3PW_{12}O_{40}{\cdot}nH_2O$, PW_{12}) and 1-butyl-3-methyl-imidazolium bromide ($C_8H_{15}N_2Br$, bmimBr). They were characterized on the aspects of structure, acidity, and catalytic activity on the esterification of *n*-butanol with acetic acid.

II. EXPERIMENTS

A. Chemical reagents

The water miscible bmimBr was synthesized and purified according to the Ref.[19]. Phosphotungstic

*Author to whom correspondence should be addressed. E-mail: chuwei1965_scu@yahoo.com

heteropolyacid (PW_{12}) was obtained from Shanghai Pharma Group Co, Ltd. and was used as received.

B. Catalyst preparation

The bmim-PW_{12} samples were synthesized as follows: PW_{12} and bmimBr were dissolved in deionized water, respectively. The bmimBr solution was slowly added into the PW_{12} solution at 40 °C with vigorous stirring, and the resulting precipitates were filtered. The white products were washed with deionized water and dried at 60 °C in vacuum. Samples were annealed under atmosphere at a temperature in the range of 100−450 °C for 3 h, and were kept at room temperature for further use. The sample was labeled as bmim-PW_{12}-T_i, for example, the bmim-PW_{12}-300 meant the sample was annealed at 300 °C.

C. Characterizations of the novel bmim-PW_{12} catalysts

The FT-IR spectra of the samples were measured using the KBr wafer in a Nicolet 5700 FT-IR spectrometer. The spectra were recorded in the range of 400−4000 cm^{-1}. X-ray diffraction (XRD) tests were performed on a X'PRO MPD diffractometer using Cu Kα radiation between 5° and 70° [20]. The voltage and anode current were 40 kV and 40 mA, respectively. The scan step was 2°/min. The thermogravimetric analysis (TGA) was conducted on a TA Q500 type thermal gravimeter analyzer in atmosphere at a rate of 10 °C/min. The sample loading was typical 25−30 mg. Scanning electron micrographs (SEM) were obtained using a Philips XL 30 electron microscope. Before the analysis, the catalysts were dissolved into ethanol and then deposited on a sample holder with a piece of adhesive carbon tape. The samples were sputtered with a thin film of gold after the ethanol was volatilized.

The specific surface area, total pore volume and average pore diameter were measured by the N_2 adsorption/desorption method with a Quantachrome Nova 1000e volumetric instrument [21] at liquid nitrogen temperature. Samples were degassed at 300 °C for 3 h prior to the analysis. The surface area was calculated by using the Brunauer-Emmett-Teller (BET) method. The total pore volume was calculated from the amount of vapor adsorbed at a relative pressure (P/P_0) close to unity.

Temperature programmed desorption (TPD) of NH_3 was used for determining the quantity and strength of the acid sites of the catalysts. Samples were firstly pretreated in flowing argon at 300 °C for 1 h. After cooling down to 120 °C in argon, each sample was kept in ammonia flow for 30 min until the saturated ammonia adsorption was attained. The temperature programmed desorption was performed by rising the sample temperature at a rate of 10 °C/min from 120 °C to 800 °C. Gas chromatography (SC-200, TCD, GC-8A) monitored the state of desorption.

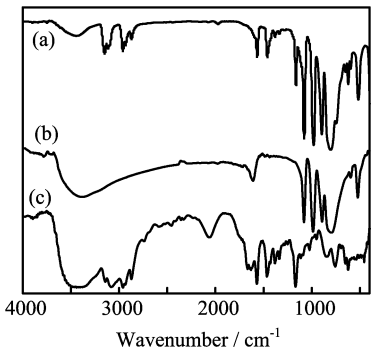

FIG. 1 FT-IR spectra of three different samples. (a) bmim-PW_{12} as synthesized, (b) PW_{12}, and (c) bmimBr.

D. Esterification reaction

In a typical reaction, *n*-butanol (0.15 mol), acetic acid (0.125 mol) and bmim-PW_{12} catalyst were placed in a 100 mL three-necked round-bottom flask fitted with a water cooled condenser. The reactions were conducted at 105 °C for 3 h. The reaction product was analyzed by the reported technique [22].

III. RESULTS AND DISCUSSION

A. Structural and surface properties of bmim-PW_{12} samples

Infrared spectra of three samples were shown in Fig.1. The Keggin anion $(PW_{12}O_{40})^{3-}$ substituted the Br^- of the bmimBr ionic liquid. In this process, PW_{12} underwent a structural transformation: three acidic protons and most of H_2O molecules were replaced by three bmimBr cations [23]. The spectrum of Keggin-type PW_{12} sample clearly showed four typical peaks in the range of 1100−700 cm^{-1} of their FT-IR spectra [24, 25]. The spectrum of bmim-PW_{12} presented characteristic absorption peaks at 1080 cm^{-1} (P−O stretching), 985 cm^{-1} (W=O stretching), 892 cm^{-1} (W−O−W_{corner} stretching), 800 cm^{-1} (W−O−W_{edge} stretching). Herein, these peaks of PW_{12} Keggin clusters in the bmim-PW_{12} sample agreed well with those of pure PW_{12} sample. This meant that the PW_{12} Keggin structure was retained during the synthetic process of bmim-PW_{12} sample.

For the pure bmimBr ionic liquid, the spectral features presented bands at 3141 cm^{-1} (C−H stretching of heterocycle), 2960 cm^{-1} (aliphatic C−H stretching), 1571 cm^{-1} (C=N stretching), 1170 cm^{-1} (heterocycle stretching) [26, 27]. The imidazolium peaks of the

DOI:10.1088/1674-0068/23/04/473-478

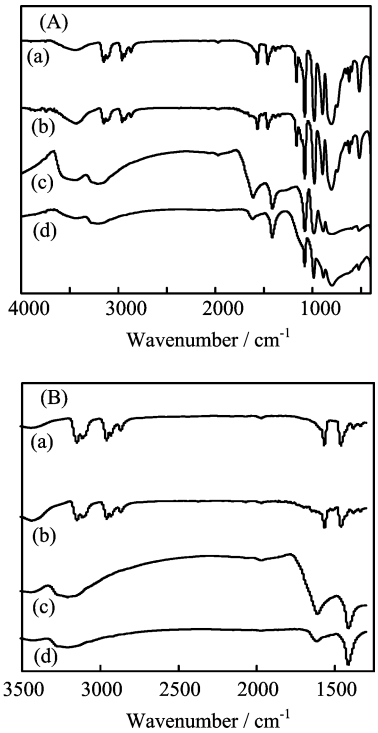

FIG. 2 (A) FT-IR spectra of bmim-PW_{12} samples, (B) the enlarge part of (A). (a) Bmim-PW_{12} as synthsized, (b) bmim-PW_{12}-200, (c) bmim-PW_{12}-400, and (d) bmim-PW_{12}-450.

bmim-PW_{12} structures had a shift of 1−7 cm^{-1} compared with those of pure bmimBr. This indicated a chemical interaction between the PW_{12} anion and the imidazolium cation.

Infrared spectra of the bmim-PW_{12} samples annealed at different temperatures were illustrated in Fig.2. Infrared spectrum of bmim-PW_{12}-200 sample was in agreement with that of bmim-PW_{12} as synthesized. The bmim-PW_{12}-400 and bmim-PW_{12}-450 samples did not show the peaks of the imidazolium heterocycle, which resulted from their partial decomposition with the increase of annealing temperature (Fig.2 (c) and (d)). Moreover, bmim-PW_{12}-400 sample showed a new bending mode of $[N(CH_3)_xH_{4-x}]^+$ at 1412 cm^{-1} [28] and the peak of $H_5O_2^+$ (the bending vibration at 1612 cm^{-1} and the stretching vibration at 3200 cm^{-1}) [29]. But the characteristic peak of $H_5O_2^+$ for bmim-PW_{12}-450 sample was very weak. This meant that the $H_5O_2^+$ was gradually lost when the annealing temperature was higher than 400 °C.

The XRD diffractions of five samples were illustrated in Fig.3. The diffraction lines turned out sharps at low angles and showed broad lumps at angles greater than 15° (2θ) for bmim-PW_{12} as syntheiszed and bmim-PW_{12}-200 sample. These features showed the long-range ordering of bmim-PW_{12} samples. With an increase of the annealing temperature, the diffractions at low angles became weak due to the disappearing of bmim-PW_{12} ordering structure (Fig.3(c)). The diffraction pattern of bmim-PW_{12}-400 sample was similar to that of pure PW_{12} (Fig.3(e)). The lower hydrates of the 12-phosphotungstic heteropoly-acid compounds generally had cubic (Pn3m) crystal structures [30]. Therefore, the conclusion could be drawn that bmim-PW_{12}-400 sample had the structure of $[N(CH_3)_xH_{4-x}]_3{\cdot}PW_{12}O_{40}$. The diffraction showed broad lumps at angles from 20° to 35° for the bmim-PW_{12}-450 sample (Fig.3(d)), which was different from that of pure PW_{12}. This indicated that the structure of bmim-PW_{12} sample would change when the annealing temperature was higher than 450 °C.

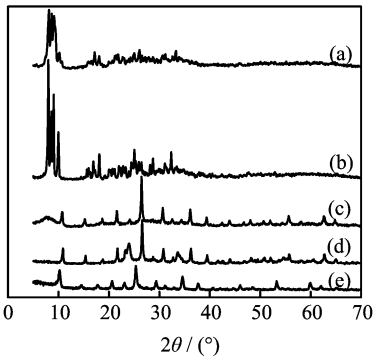

FIG. 3 XRD patterns of five samples: (a) bmim-PW_{12} as synthsized, (b) bmim-PW_{12}-200, (c) bmim-PW_{12}-400, (d) bmim-PW_{12}-450, and (e) pure PW_{12}.

TABLE I Physico-chemical properties including surface area S, pore volume V, pore diameter d, particle size l.

Sample	$S/(m^2/g)$	$V/(\mu L/g)$	d/nm	l/nm
bmim-PW_{12}	0.604	2.65	–	–
bmim-PW_{12}-400	5.28	6.44	4.88	28.0

The particle sizes of these samples were calculated by Scherrer formula, which are shown in Table I. Because of unclear crystal structure for bmim-PW_{12} as synthesized, it was difficult to calculate the particle diameter. For bmim-PW_{12}-400 sample which had the phase structure of $[N(CH_3)_xH_{4-x}]{\cdot}_3PW_{12}O_{40}$, the particle size was only 28 nm. The results indicated that the nano-sized composites based on functionalized acidic ionic liquid were prepared when the bmim-PW_{12} samples were annealed at 400 °C.

Figure 4 displayed the TG-DTG curve for the bmim-PW_{12} sample. The TG curve illustrated a three-step weight loss, which was in agreement with that reported in the Ref.[31]. The first step was assigned to the mass loss of the physisorbed and structural water when the temperature was below 300 °C. The maximum rate of weight loss at about 180 °C was corresponding to the peak in DTG curve. The second one began at the temperature of 300 °C, which was due to the decomposition

DOI:10.1088/1674-0068/23/04/473-478

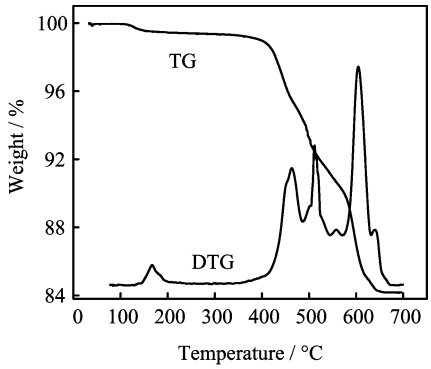

FIG. 4 TG-DTG profiles of bmim-PW_{12} sample.

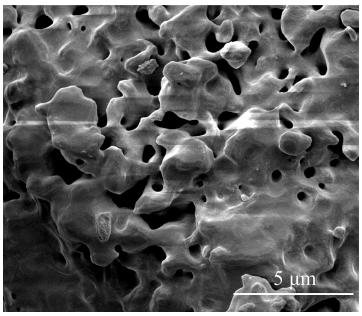

FIG. 5 SEM image of bmim-PW_{12}-400.

of the organic part. There were three maximum rate of weight loss at about 445, 495, and 545 °C, respectively. The last loss was assigned to the decomposition of bmim-PW_{12} Keggin structure, corresponding to the loss peak in DTG curve at about 600 °C. It was the highest weight loss of the sample.

Figure 5 showed the top-view SEM image of the sample annealed at 400 °C. There were lots of pores irregularly dispersing on the surface of bmim-PW_{12}-400 sample. This meant that the porous functionalized acidic ionic liquid was synthesized when the bmim-PW_{12} sample was annealed at 400 °C.

B. Catalytic performance and re-usability of the novel bmim-PW_{12} catalyst

The yield of butyl acetate catalyzed by different catalysts was displayed on Table II. The yield was only 35.1% without any catalyst. High yield of 93.2% was obtained for the PW_{12} homogeneous catalyst with strong acidity. But it was difficult to be separated after reaction. There was little catalytic activity for the bmimBr ionic liquid catalyst. The yield was up to 90.6% for the bmim-PW_{12}-400 catalyst. The bmim-PW_{12} ionic liquid catalyst was insoluble in alcohol, acids, esters, *etc.* and could be a heterogeneous catalyst for esterification reaction [32]. In the references, the active component loaded on carrier was mainly through physical adsorption for the traditional catalyst which led to weak force, low activity, and easy to dissolve [33]. However, this kind of catalyst (bmim-PW_{12}-400) had a high activity and a good re-utilization.

TABLE II The ester yield for several catalysts. Reaction: 105 °C, 3 h, reaction catalyst amount: 5%.

Catalyst	Phenomenon	Ester yield/%
No catalyst	–	35.1
BmimBr	Homogeneous	35.2
PW_{12}	Homogeneous	93.2
Bmim-PW_{12}-400	Heterogeneous	90.6

TABLE III Effect of annealed temperature of bmim-PW_{12} sample on the ester yield. Reaction: 105 °C, 3 h, reaction catalyst amount: 5%.

Catalyst	Annealed temp./°C	Ester yield/%
Bmim-PW_{12}-100	100	41.8
Bmim-PW_{12}-200	200	36.5
Bmim-PW_{12}-300	300	35.5
Bmim-PW_{12}-350	350	82.8
Bmim-PW_{12}-400	400	90.6
Bmim-PW_{12}-450	450	47.9

Table III illustrated the effect of annealing temperature on the ester yield. The annealing temperature possessed important influence on the catalytic performance. There was a slight decrease on the yield with the annealing temperature increasing below 350 °C. But when the temperature was up to 350 °C, the yield increased remarkably. The ester yield reached the highest value of 90.6% when the annealing temperature was 400 °C. The ester yield catalyzed by bmim-PW_{12}-400 sample was more than two times of that catalyzed by bmim-PW_{12}-100 catalyst. The reason should be that as the annealing temperature increased, the organic part of the bmim-PW_{12} catalyst partly decomposed and the new nano-porous substance ($[N(CH_3)_xH_{4-x}]_3{\cdot}PW_{12}O_{40}$) was generated, which could absorb $H_5O_2^+$ as acidic protons (seen by FT-IR) for acid catalyzed reaction [34]. When the annealed temperature of bmim-PW_{12} catalyst further increased to 450 °C, the ester yield decreased obviously due to that the $H_5O_2^+$ were gradually lost.

The effect of mass ratio of bmim-PW_{12}-400 catalyst on the yield of butyl acetate was also discussed, which was shown in Fig.6. The ester yield increased rapidly with the mass increase of bmim-PW_{12} -400 catalyst and reached a high value of 90.6% at 5%. There was only a slight increase of the ester yield as the catalyst amount increased more than this amount value.

The re-usability of bmim-PW_{12}-400 catalyst was illustrated in Fig.7. For the fresh sample, the bmim-PW_{12}-400 catalyst showed a very high activity. How-

DOI:10.1088/1674-0068/23/04/473-478

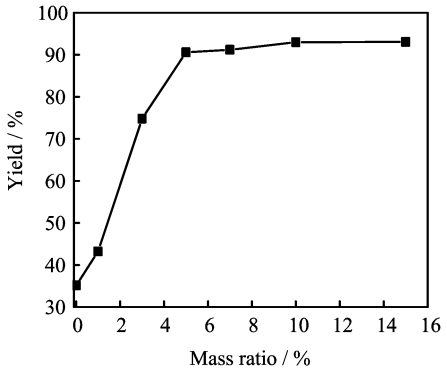

FIG. 6 Effect of the mass ratio* of bmim-PW_{12}-400 catalyst on the ester yield. Reaction conditions: 100−105 °C, 3 h.

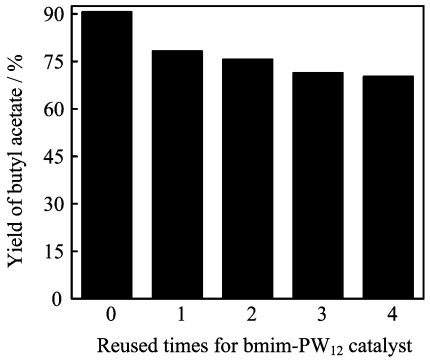

FIG. 7 Re-usability of the bmim-PW_{12}-400 catalyst. Reaction conditions: 105 °C, 3 h, catalyst amount of 5%.

ever, the yield of butyl acetate decreased slightly when the catalyst was secondly used. There were very slight differences on the ester yield when the catalyst was further reused. The catalytic activity slightly decreased, which was resulted from the high adsorptivity of the final products on the surface of the bmim-PW_{12} catalyst [31].

C. Texture and acidic properties of bmim-PW_{12} samples

Table I showed the texture properties of the bmim-PW_{12} as synthesized and bmim-PW_{12}-400 sample using N_2-adsorption/desorption method. There was almost no pore and the surface area was very small for bmim-PW_{12} as synthesized. But there was a large increase for the surface area and the pore diameter of bmim-PW_{12}-400 catalyst. The pore diameter of the bmim-PW_{12}-400 sample was up to 4.88 nm. Considering the size and shape of the heteropoly anion and the crystal structure of $[N(CH_3)_xH_{4-x}]_3{\cdot}PW_{12}O_{40}$ (28 nm), there was no open pore in the crystal structure through which an nitrogen molecule (0.36 nm in diameter) can penetrate. Thus, the pore of catalyst described here were interparticle, not intracrystalline [29]. The crystal structure

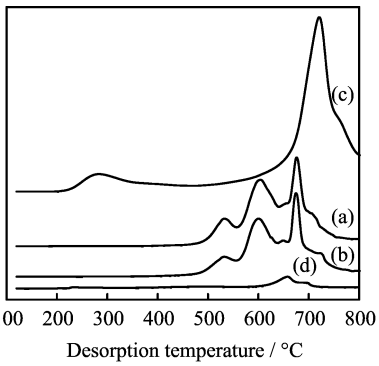

FIG. 8 NH_3-TPD profiles of four catalysts. (a) Bmim-PW_{12} as synthesized, (b) bmim-PW_{12}-200, (c) bmim-PW_{12}-400, (d) bmim-PW_{12}-450.

of bmim-PW_{12}-400 catalyst was as the same as that of the cubic PW_{12} which was divided into three classes of structures (primary structure, secondary structure, and tertiary structure). Therefore, the secondary structure of bmim-PW_{12}-400 catalyst was three-dimensional arrangement consisting of large polyanions (primary structure), cations, crystal waters (seen from FT-IR spectra). The assemblage of the secondary structure formed into tertiary structure and in this process the pores were generated [29].

The acid properties including acidic sites amount and acid strength of bmim-PW_{12} catalysts annealed at several temperatures were evidenced by NH_3-TPD, and which were shown in Fig.8. In the NH_3-TPD curves, peaks were generally distributed into two regions, below and above 400 °C referred to low-temperature (LT) and high-temperature (HT) region, respectively [34, 35]. The peaks in the HT and LT regions can be attributed to the NH_3 desorption at strong and weak acid sites, respectively. It could be found that the peaks only appeared in the high-temperature region for the bmim-PW_{12} as synthesized and bmim-PW_{12}-200 sample. The acid strength of weak acidic sites increased markedly for bmim-PW_{12}-400 sample, which indicated that new acid sites might be generated on surface. The reason should be that the imidazolium cation was partly decomposed and the new structure of $[N(CH_3)_xH_{4-x}]_3{\cdot}PW_{12}O_{40}$ could absorb $H_5O_2^+$ as acidic protons [23]. As the annealing temperature further increased, the weakly acidic sites almost disappeared for the catalyst annealed at 450 °C, while the strongly acidic sites were also decreased markedly compared to those of the catalyst annealed at 400 °C.

From the peak areas, the bmim-PW_{12} as synthesized and bmim-PW_{12}-200 sample had the similar acid amount. The number of weak acidic sites and strong acidic sites of bmim-PW_{12}-400 sample was obviously more than those of other catalysts. The number of strong acidic sites of bmim-PW_{12}-450 sample was the lowest of all catalysts due to the gradual lost of $H_5O_2^+$.

DOI:10.1088/1674-0068/23/04/473-478

IV. CONCLUSION

Novel functionalized ionic liquid samples were synthesized and were annealed at 100−450 °C. The structure of bmim-PW_{12}-400 sample was estimated to be $[N(CH_3)_xH_{4-x}]_3{\cdot}PW_{12}O_{40}$. The bmim-$PW_{12}$ samples kept Keggin structure and had excellent catalytic activity on esterification reaction especially when the bmim-PW_{12} sample had been annealed at 400 °C.

The IR, NH_3-TPD, and XRD results, show that bmim-PW_{12}-400 composite exhibited porous structure, nano particles, strong acidity, and excellent catalytic activity on the ester yield. This was due to the decomposition of the organic part, the crystallization of bmim-PW_{12}-400 composite and the increase of adsorbed and/or structural $H_5O_2{}^+$ on bmim-PW_{12}-400 sample. On the basis of the findings of this work, the exploration of the catalysts in other reactions and altering the composition of the catalysts is in progress.

V. ACKNOWLEDGMENT

This work was supported by the National Basic Research Program of China (No.2007CB936800).

[1] J. Dupont, R. F. D. Souza, and P. A. Z. Suarez, Chem. Rev. **102**, 3667 (2002).
[2] J. H. Li, Y. F. Shen, Y. J. Zhang, and Y. Liu, Chem. Commun. 360 (2005).
[3] K. R. Seddon, J. Chem. Tech. Biotechnol. **68**, 351 (1997).
[4] D. B. Zhao, M. Wu, Y. Kou, and E. Z. Min, Catal. Today **74**, 157(2002).
[5] P. Wasserscheid and W. Keim, Angew. Chem. Int. Ed. **39**, 3772 (2000).
[6] T. Welton, Coord. Chem. Rev. **248**, 2459 (2004).
[7] S. V. Dzyuba and R. A. Bartsch, Angew. Chem. Int. Ed. **42**, 148 (2003).
[8] R. Seddon, Chem. Comm. 2399 (2001).
[9] L. Dai, S. Yu, Y. Shan, and M. He, Eur. J. Inorg. Chem. 237 (2004).
[10] A. B. Bourlinos, K. Raman, R. Herrera, Q. Zhang, L. A. Archer, and E. P. Giannelis, J. Am. Chem. Soc. **126**, 15358 (2004).
[11] P. G. Rickert, M. R. Antonio, M. A. Firestone, K. A. Kubatko, T. Szreder, J. F. Wishart, and M. L. Dietz, J. Phys. Chem. B **111**, 4685 (2007).
[12] M. H. Chiang, J. A. Dzielawa, M. L. Dietz, and M. R. Antonio, J. Electroanal. Chem. **567**, 77 (2004).
[13] J. D. Kim, S. Hayashi, T. Mori, and I. Honma, Electrochimica Acta **53**, 963 (2007).
[14] R. C. Larock, *Comprehensive Organic Transformations*, New York: VCH, 14 (1999).
[15] W. Chu, J. P. Hu, Z. K. Xie, and Q. L. Chen, Catal. Today **90**, 349 (2004).
[16] K. Nagasawa, K. Ohhashi, A. Yamishita, and K. Ito, Chem. Lett. **23**, 209 (1994).
[17] R. A. Sheldon and R. S. Downing, Appl. Catal. A **189**, 163 (1999).
[18] P. Tundo and P. T. Anastas, Eds., *Green Chemistry: Challenging Perspectives*, Oxford: Oxford University Press 24 (1999).
[19] J. G. Huddleston, A. E. Visser, W. M. Reichert, H. D. Willauer, G. A. Broker, and R. D. Rogers, Green Chem. **3**, 156 (2001).
[20] A. Khodahov, W. Chu, and P. Fongarland, Chem. Rev. **107**, 1692 (2007).
[21] J. Q. Xu, W. Chu, and S. Z. Luo, J. Mol. Catal. A **256**, 48 (2006).
[22] H. Li, *Experimental Organic Chemistry*, Beijing: Chemical Industry Press, 24 (2007).
[23] Z. Y. Li, Q. Zhang, H. T. Liu, P. He, X. D. Xu, and J. H. Li, J. Power Sources **158**, 103 (2006).
[24] I. Honma, H. Nakajima, O. Nishikawa, T. Sugimoto, and S. Nomura, Solid State Ionics **237**, 162 (2003).
[25] M. Misono, Catal. Rev. Sci. Eng. **29**, 269 (1987).
[26] M. Koel, Proc. Estonian Acad. Sci. Chem. **49**, 145 (2000).
[27] S. Tait and R. A. Osteryoung, Inorg. Chem. **23**, 4352 (1984).
[28] K. Nakamoto, *Infrared and Raman Spectra of Inorganic and Coordination Compounds*, Part A, 5th Ed., Wiley-Interscience, 191 (1997).
[29] N. Mizuno and M. Misono, Chem. Rev. **98**, 199 (1998).
[30] J. B. Moffat and S. Kasztelan, J. Catal. **109**, 206 (1988).
[31] J. H. Shi and G. Pan, Chin. J. Catal. **29**, 629 (2008).
[32] Y. Leng, J. Wang, D. R. Zhu, X. Q Ren, H. Q. Ge, and L. Shen, Angew. Chem. Int. Ed. **48**, 168 (2009).
[33] M. M. Heravi and S. Sadjadi, J. Iran Chem. Soc. **6**, 1 (2009).
[34] C. A. Emeis, J. Catal. **141**, 347 (1993).
[35] M. Sawa, M. Niwa, and Y. Murakami, Zeolites **10**, 532 (1990).

DOI:10.1088/1674-0068/23/04/473-478